Miner Deposita (2006) 41: 599–606
DOI 10.1007/s00126-006-0081-7

LETTER

Hong Zhong · Wei-Guang Zhu

Geochronology of layered mafic intrusions from the Pan–Xi area in the Emeishan large igneous province, SW China

Received: 25 October 2005 / Accepted: 20 June 2006 / Published online: 15 August 2006

Abstract The Panzhihua–Xichang (Pan-Xi) area hosts mafic/ultramafic intrusions, which are part of the Permian Emeishan large igneous province. Some of these intrusions host giant Fe–Ti–V deposits and minor Ni–Cu–PGE mineralization. In the present study, zircon U–Pb ages of 259.3±1.3 and 260.7±0.8 Ma have been obtained from the giant Fe–Ti–V ore-bearing Hongge and the unmineralized Binggu intrusions, respectively, by isotope dilution thermal ionization mass spectrometry method. In combination with the ages of other ore-bearing intrusions, this age shows that these mafic/ultramafic intrusions were emplaced at ca. 260 Ma. The Hongge and Binggu intrusions cut the lower part of the rapidly deposited Emeishan flood basalt sequence but no further into the upper volcanic sequence in the Pan-Xi area. Thus, emplacement and mineralization of the mafic/ultramafic intrusions were almost contemporaneous with the eruption of the Emeishan flood basalts during a relatively short time span.

Keywords Geochronology · Layered intrusions · Emeishan large igneous province · Ni–Cu–PGE mineralization · China

Introduction

The Emeishan large igneous province (ELIP) in SW China, consisting of massive flood basalts and numerous associated intrusions of mafic/ultramafic to felsic compositions, has been linked to a mantle plume active near the Permo–Triassic boundary (Chung and Jahn 1995; Chung et al. 1998; Xu et al. 2001, 2004; Song et al. 2001; Zhou et al. 2002; Lo et al. 2002; He et al. 2003; Guo et al. 2004; Fan et al. 2004). Some of the mafic/ultramafic intrusions in the central part of the ELIP contain giant Fe–Ti–V–(PGE) deposits (Fig. 1, Panzhihua, Hongge, Baima, and Taihe; Yao et al. 1993; Zhong et al. 2002 and references therein) and many contain Ni–Cu–(PGE) sulfide deposits (Liang et al. 1998; Zhou et al. 2002; Zhong et al. 2002, 2004; Song et al. 2003).

The age and duration of magmatism in the ELIP have been a matter of extensive debate, concerning the main eruption stages and the suspected causal relation with the end Permian mass extinction event (e.g., Stanley and Yang 1994). Early K–Ar, Rb–Sr, and Sm–Nd dating produced ages ranging from 210 to 343 Ma for the Emeishan basalts and the mafic/ultramafic intrusions (Yuan et al. 1985; Cong 1988; Zhang et al. 1999), although some are considered unreliable. Recently, several $^{40}Ar/^{39}Ar$ dates of 42–256 Ma with complicated age spectra were reported for the Emeishan basalts, the younger ages representing Mesozoic and Cenozoic overprints (Boven et al. 2002; Lo et al. 2002; Ali et al. 2004). SHRIMP zircon U–Pb ages of 259±3 (Zhou et al. 2002), 263±3 and 262±2 Ma (Zhou et al. 2005), and 262±3 Ma (Guo et al. 2004) were recently obtained for the Xinjie, Panzhihua and Baima mafic/ultramafic intrusions (Fig. 1), and for the Yanyuan diabasic dike in the Panzhihua–Xichang (Pan-Xi) area, respectively, which are considered to be the associated products of the ELIP. However, correlations have been poorly made between the above-mentioned mafic/ultramafic intrusions and the flood basalt sequence.

In this paper, more precise ages of the giant ore-bearing Hongge and unmineralized Binggu intrusions in the Pan-Xi area, which were emplaced into the volcanic cycle II of the Emeishan basalts and are geochemically associated with the basalts, were obtained by using U–Pb isotope dilution thermal ionization mass spectrometry. The objectives of this study were to determine the emplacement ages of the mineralized and nonmineralized mafic/ultramafic intrusions and to place temporal constraints on the main mineralization event associated with the ELIP.

Editorial handling: M. Chiaradia

H. Zhong (✉) · W.-G. Zhu
State Key Laboratory of Ore Deposit Geochemistry,
Institute of Geochemistry, Chinese Academy of Sciences,
46 Guanshui Road,
Guiyang, 550002, People's Republic of China
e-mail: zhonghong@vip.gyig.ac.cn
Tel.: +86-851-5891820
Fax: +86-851-5891664

Fig. 1 Geological map of the Pan-Xi area showing the position of Permian layered intrusions (modified after Liu et al. 1985; Cong 1988). The SHRIMP zircon U/Pb age of the Xinjie intrusion is from Zhou et al. (2002), and the SHRIMP zircon U/Pb ages of the Panzhihua and Baima intrusions are from Zhou et al. (2005). The *inset map* illustrates the distribution of major terranes in China (the *shaded area* indicates the distribution of the Emeishan basalts; modified after Chung and Jahn 1995). *NCB* North China block, *YZB* Yangtze block, *SG* Songpan-Ganze accretionary complex, *QT* Qiangtang, *LS* Lhasa, *HI* Himalayan, *TAR* Tarim, *MON* Mongolia, *QD* Qaidam, *WB* West Burma, *STM* Shan–Thai–Malay, *IC* Indochina

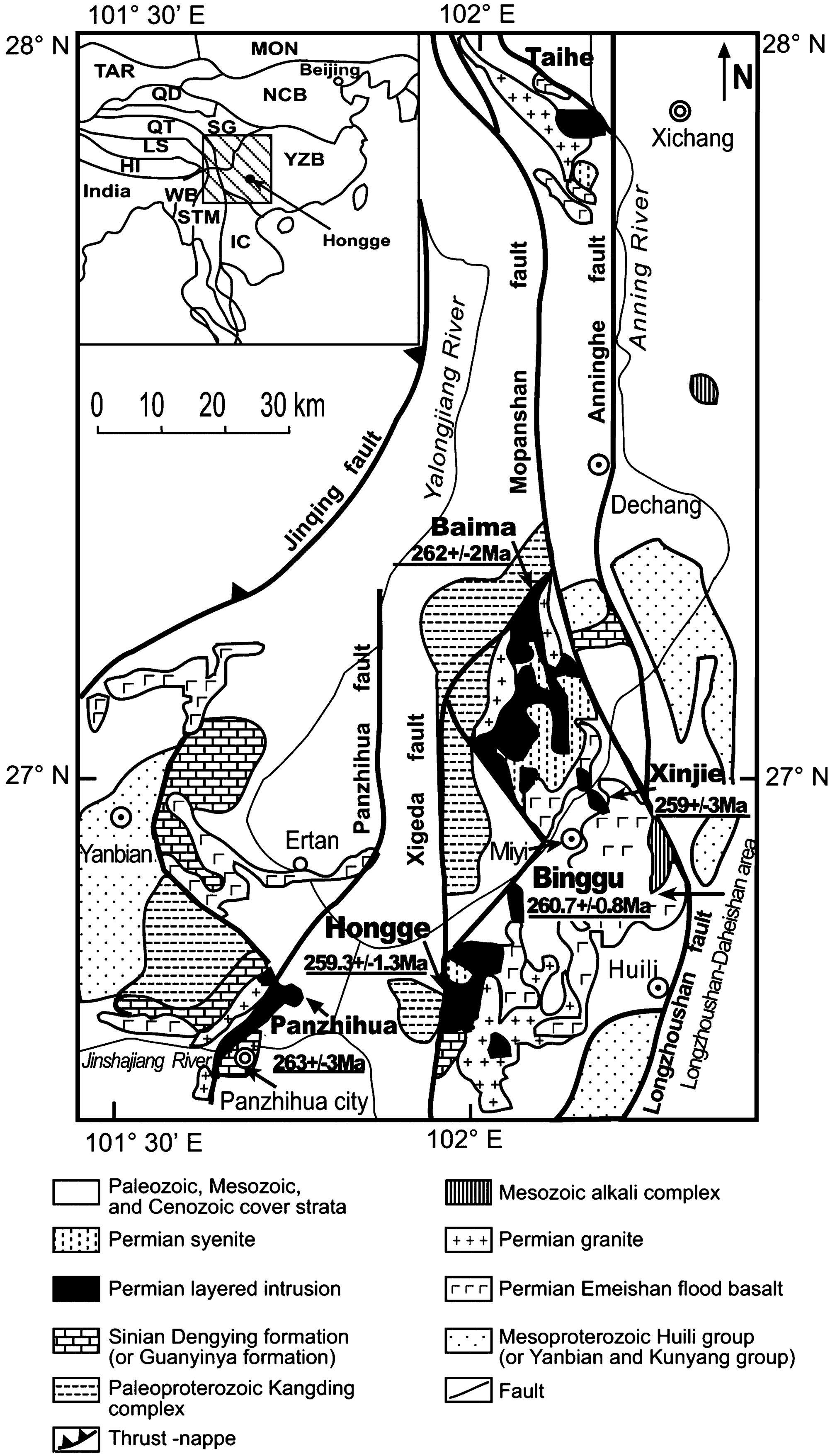

Geological background

The ELIP, comprising massive volcanic rocks, numerous ultramafic/mafic intrusive rocks, granites, and syenites, is exposed over a large part of SW China, from the eastern margin of the Tibetan Plateau to the western margin of the Yangtze block (Fig. 1). The extensive ELIP is believed to result from mantle plume activity (e.g., Chung and Jahn 1995; Chung et al. 1998; Xu et al. 2001), although, earlier, it was thought to be related to stable cratonic rifting (e.g., Luo et al. 1990).

The Emeishan basalts, correlated with the mafic/ultramafic intrusions in this paper, are located in the Longzhoushan and Daheishan area in the central part of the ELIP (Fig. 1). The volcanic formation is composed of four cycles, with basaltic volcanic (agglomerate) breccia and lapilli tuff at the bottom of each cycle. The thickness ranges from several hundred meters up to 5 km (BGMRSP 1995). From the bottom part of the formation, cycle I is mainly composed of (olivine) pyroxene-phyric, amygdaloidal basalts interbedded with massive plagioclase-phyric basalts and basaltic volcanic breccia. Cycle II predominantly consists of massive, amygdaloidal (olivine) pyroxene-phyric basalts intercalated with plagioclase-phyric basalts. Cycle III is mainly composed of massive, amygdaloidal plagioclase-phyric basalts interbedded with (olivine) pyroxene-phyric basalts, basaltic breccias (tuffs), and basaltic volcanic breccias (tuffs), and cycle IV mainly consists of massive, plagioclase-phyric basalts, and amygdaloidal basalts and andesites.

The mafic/ultramafic intrusions occur predominantly along a 300-km long belt, which is controlled by regional N–S trending faults (Liu et al. 1985; Cong 1988) in the Pan-Xi area (Fig. 1). Some of the intrusions are well-known in China because of their Fe–Ti–V deposits and Ni–Cu–PGE mineralization. For example, the Panzhihua, Hongge, Taihe, and Baima intrusions contain giant Fe–Ti–V deposits (Fig. 1). The Hongge and Xinjie mafic/ultramafic intrusions contain major PGE-rich horizons in their lower parts (Liang et al. 1998; Zhong et al. 2002; Zhong et al. 2004).

Petrological features of the mafic/ultramafic intrusions

The Hongge layered intrusion crops out over an area of about 60 km^2 and intruded the Mesoproterozoic Huili Group consisting of low-grade metasedimentary rocks intercalated with minor metavolcanic rocks (SBGMR 1991). The intrusion occurred along the N–S striking Xigeda fault, whereas the emplacement of the adjacent Emeishan basalts occurred between the regional Longzhoushan and Xigeda faults (Fig. 1). The Hongge intrusion was emplaced into rocks of volcanic cycle II of the four cycles for the neighboring Emeishan basalts in the Daheishan area, but cut no further into the upper volcanic sequence (SBGMR 1991; BGMRSP 1995; Ma et al. 2001). It also contains partially greenschist-facies metamorphosed basalt xenoliths, whereas numerous geochemically similar, mafic dikes cut the lower suites of the basalts, indicating that the Hongge intrusion is slightly younger than the basalts from the lower volcanic sequence (SBGMR 1991).

The intrusion occurs in coincidence with the location of the maximum thickness of comagmatic lavas (Zhong et al. 2005). The Permian granites intruded the Hongge intrusion and the adjacent Emeishan basalts, and the Permian syenites were also emplaced into the Hongge intrusion (Fig. 1).

The Hongge intrusion has well-developed igneous layering and consists of three zones: the lower olivine–clinopyroxenite zone (LOZ), the middle clinopyroxenite zone (MCZ), and the upper gabbro zone (UGZ) (Zhong et al. 2002). The LOZ and UGZ are delineated by single compositional cyclic units, whereas the MCZ has two compositional cyclic units (Fig. 2a).

The Hongge Fe–Ti–V deposit is the second largest economic concentration of iron and titanium of this type in China, with only the Panzhihua deposit in the Pan-Xi area being larger. It is also the largest in terms of contained vanadium reserves (Yao et al. 1993; Zhong et al. 2005). The intrusion contains 1.83×10^9 t Fe, 1.96×10^8 t Ti, and 1.45×10^7 t V, with ore grading 27.04 wt% FeO_T (total Fe), 10.57 wt% TiO_2, and 0.24 wt% V_2O_5 (Yao et al. 1993). The MCZ and UGZ host layers of disseminated V- and Ti-rich magnetite that are 14 to 84 m thick and 300 to 1,700 m long, of which those in the MCZ form the most important deposits (Fig. 2a; Yao et al. 1993; Zhong et al. 2002). The PGE-enriched horizons in the lower parts of the LOZ and MCZ are associated with Cu- and Ni-rich sulfides (Fig. 2a; Liang et al. 1998; Zhong et al. 2002).

The poorly studied and unmineralized Binggu intrusion is a 7-km long by 1- to 1.5-km wide mafic sill, which was also emplaced into the volcanic cycle II of the adjacent Emeishan basalts in the Longzhoushan area and contains basalt fragments from the volcanic cycle II (Fig. 2b; BGMRSP 1995). The Binggu intrusion, is composed of three cycles, which are, from bottom to top, olivine gabbro cycle (cycle I), norite–gabbro cycle (cycle II), and hornblende gabbro cycle (cycle III) (Fig. 2b).

Sampling and analytical methods

Sample HGF-01 is a mineralized gabbro, collected from the lower part of the UGZ in the Hongge intrusion (Fig. 2a). Sample DS-01 is a hornblende gabbro, collected from the nonmineralized hornblende gabbro unit (cycle III) of the Binggu intrusion (Fig. 2b). Zircons were extracted from 20-kg samples using standard techniques of density and magnetic separation.

Separated zircons grains were cleaned thoroughly in warm concentrated HNO_3 for about 1 hour and then in deionized water. The chemical procedures are similar to those of Krogh (1973, 1982). Washed and weighed zircons were dissolved with double-distilled concentrated HF for about 48 h at 195°C in Teflon Bomb and spiked with a mixed $^{205}Pb/^{235}U$ tracer solution. The spiked solutions

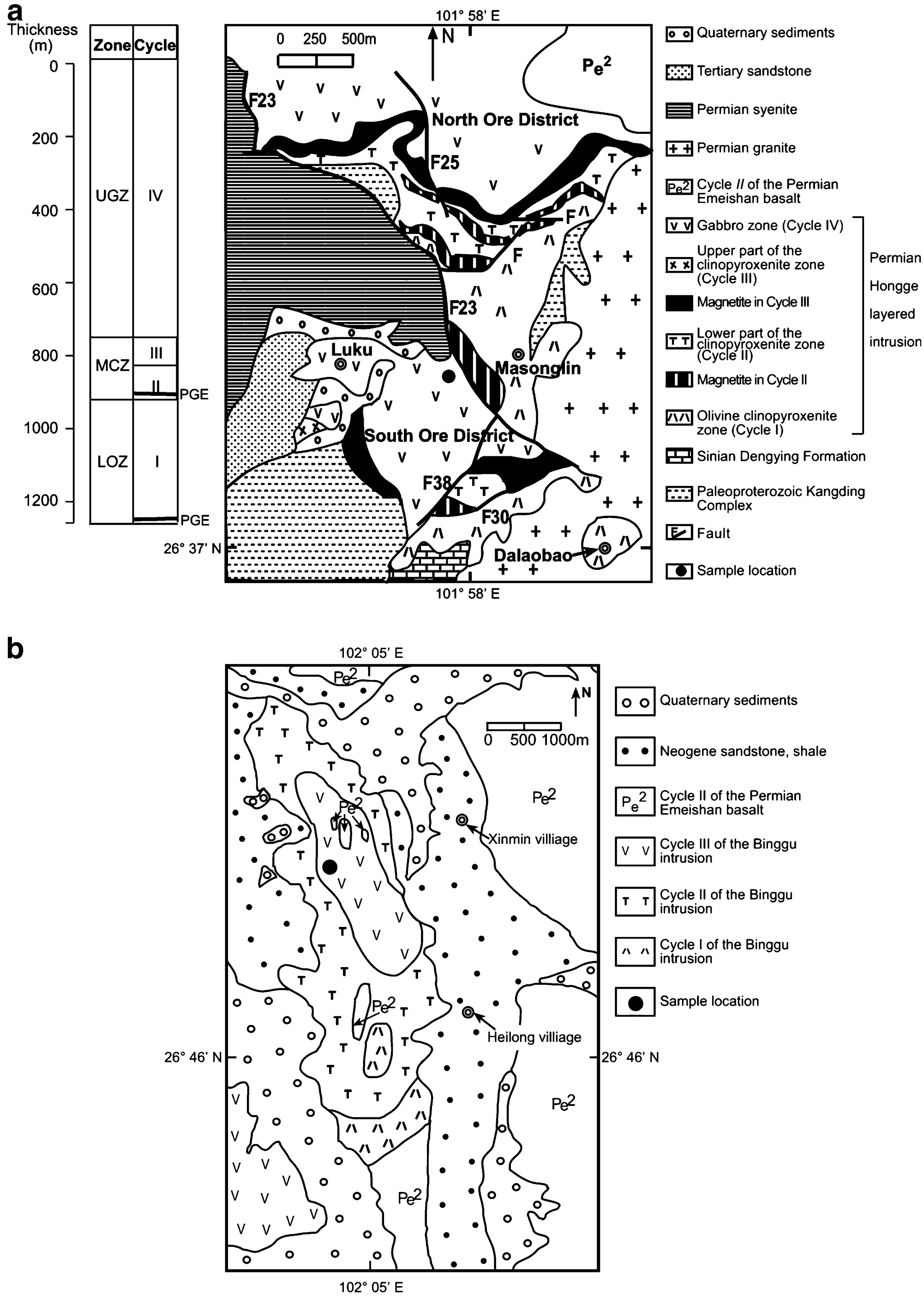

Fig. 2 **a** Simplified stratigraphy and geological map of the Hongge intrusion (modified after Zhong et al. 2002). *UGZ* Upper gabbro zone, *MCZ* middle clinopyroxenite zone, *LOZ* lower olivine clinopyroxenite zone, *I–IV* cycles I–IV. *Dark bands* at base of sections II and I in the *Cycle column* indicate PGE-enriched layers. **b** Simplified geological map of the Binggu intrusion (modified after unpublished map of BGMRSP 1995)

were evaporated to incipient dryness and loaded on an outgassed single Re filament with silica gel and phosphoric acid. Total procedural blanks were usually about 15–50 pg for Pb and <2 pg for U; blank isotopic composition is $^{206}Pb/^{204}Pb=17.97\pm1.0$, $^{207}Pb/^{204}Pb=15.55\pm0.5$, and $^{208}Pb/^{204}Pb=37.71\pm1.5$ (all 2σ of population). Initial common Pb in excess of the blank was corrected according to the Stacey–Kramers Pb evolution model. U–Pb isotope analyses were conducted using a VG-354 thermal ionization mass spectrometer at the Tianjin Institute of Geology and Mineral Resources, China. A fractionation correction of 0.10% per atomic mass unit for both Pb and U was used. Corrections for fractionation and dead time were determined using replicate analyses of NIST standards NBS982 and U-500. $^{206}Pb/^{204}Pb$ ratios have been corrected for fractionation and spike. All other isotopic ratios have been corrected for fractionation, spike, blank, and initial common Pb. Age and error propagation calculations were made using the ISOPLOT program version 3.20 of Ludwig.

Table 1 U/Pb isotope dilution analytical results for zircons from the Hongge and Binggu intrusions

No.	Properties	Wt (μg)	U (ppm)	Pb (ppm)	PbC (ng)	Isotopic ratios						Age (Ma)		
						$^{206}Pb/^{204}Pb$	$^{208}Pb/^{206}Pb$	$^{206}Pb/^{238}U$	$^{207}Pb/^{235}U$	Rho	$^{207}Pb/^{206}Pb$	^{206}Pb ^{238}U	$^{207}Pb/^{235}U$	$^{207}Pb/^{206}Pb$
HGF-01														
1	py, cl, i	20	724	36	0.039	972	0.2978	0.04102±50	0.2906±52	0.751	0.05138±61	259.2±3.2	259.1±4.0	258±27
2	py, cl, i	40	1,335	68	0.220	648	0.2770	0.04099±33	0.2914±33	0.773	0.05156±37	259.0±2.1	259.6±2.7	266±16
3	pyb, cl, sp, e	40	779	42	0.150	572	0.3525	0.04107±47	0.2910±49	0.746	0.05139±58	259.4±3.0	259.3±3.9	258±26
4	pyb, cl, sp, e	30	975	49	0.046	1,660	0.3154	0.04117±51	0.2924±53	0.755	0.05151±61	260.1±3.2	260.4±4.2	264±27
5	c, cl, i	20	480	52	0.600	60	0.2696	0.04086±105	0.2876±145	0.633	0.05105±202	258.2±6.7	257±11	243±91
DS-01														
6	pyb, cl, i	80	1,011	56	0.720	314	0.2494	0.04147±21	0.2947±21	0.762	0.05155±24	261.9±1.3	262.3±1.7	265±11
7	pyb, cl, sp, e	80	852	52	1.000	195	0.2626	0.04132±24	0.2942±25	0.757	0.05164±29	261.0±1.5	261.9±2.0	270±13
8	pyb, cl, sp, e	80	1,614	77	0.240	1,404	0.2495	0.04087±30	0.2904±24	0.883	0.05153±20	258.2±1.9	258.9±1.9	265±9
9	pyb, cl, i	30	3,127	172	0.770	339	0.2677	0.04137±41	0.2931±47	0.674	0.05138±61	261.3±2.6	261.0±3.7	258±27
10	pyb, cl, i	40	3,707	213	1.300	303	0.3157	0.04101±31	0.2908±72	0.363	0.05143±119	259.2±2.0	259.2±5.7	260±53

c Colorless, *cl* clear, *e* euhedral, *i* irregular, *py* pale yellow, *pyb* pale yellow-brown, *sp* short prismatic, *PbC* common Pb, *Wt* weight

$^{206}Pb/^{204}Pb$ ratios have been corrected for fractionation and spike. All other isotopic ratios have been corrected for fractionation, spike, blank, and initial common Pb. All errors are 2σ.

Analytical results

U–Pb zircon data for the gabbros from the Hongge and Binggu intrusions are given in Table 1 and plotted in Fig. 3.

Zircons in sample HGF-01 range from clear, pale yellow, irregular grains to pale yellow brown, short prismatic, colorless, irregular grains. All the five concordant and equivalent analyses yield a concordia age of 259.3±1.3 Ma (MSWD=0.27; Fig. 3a). This age is identical to the weighted mean $^{206}Pb/^{238}U$ age of 259.3±1.3 Ma (MSWD=0.112). Although fraction 5 is characterized by a high common Pb concentration, the recalculated weighted mean age (without fraction 5) is still 259.3±1.3 Ma (MSWD=0.113). Because of the young age, small size, and relatively high common Pb concentration, the error on the $^{207}Pb/^{206}Pb$ age is quite large. Despite this fact, the weighted mean of all five $^{207}Pb/^{206}Pb$ ages is 263±11 Ma, in good agreement with the weighted mean $^{206}Pb/^{238}U$ age. Thus, the best estimate for the absolute age of mineralization in the Hongge intrusion is the concordia age of 259.3±1.3 Ma.

Zircons recovered from sample DS-01 included two fractions of clear, pale yellow brown, short prismatic grains, and three fractions of clear, pale yellow brown, irregular grains. All the five equivalent concordant analyses obtained a concordia age of 260.7±0.8 Ma (MSWD=1.5; Fig. 3b). These results give $^{206}Pb/^{238}U$ ages that range from 258.2 to 261.9 Ma (Table 1) with a mean age of 260.3±1.8 Ma (MSWD=3.36; Fig. 3b), which is indistinguishable from the concordia age within analytical errors. The corresponding $^{207}Pb/^{206}Pb$ ratios agree to within analytical precision and yield a mean age of 265.6±5.8 Ma. As a result, the concordia age of 260.7±0.8 Ma can be interpreted as the crystallization age of the Binggu intrusion.

Ages of gabbros from the Hongge and Binggu intrusions are equivalent within analytical uncertainty, indicating that the two intrusions were emplaced synchronously at~260 Ma.

Discussion and conclusions

The closet link of magma-associated ore deposits with mantle plumes is represented by the large layered intrusions and associated flood basalts (Pirajno 2004). The large mafic/ultramafic layered intrusions in the Pan-Xi area are typical examples hosting giant Fe–Ti–V oxide deposits and PGE–Ni–Cu-rich sulfide mineralization (Zhong et al. 2002, 2004, 2005; Zhou et al. 2002). The presented U–Pb zircon data suggest that the ore-bearing Hongge and the unmineralized Binggu intrusions were formed synchronously at ca. 260 Ma. These results are identical, within analytical errors, to the ages of Zhou et al. (2002; 2005) and Guo et al. (2004) for other mafic/ultramafic layered intrusions and dikes with geological and geochemical similarities, which define a major mafic intrusive stage of the ELIP at 259–263 Ma. In combination with these ages, it can be concluded that the mineralized

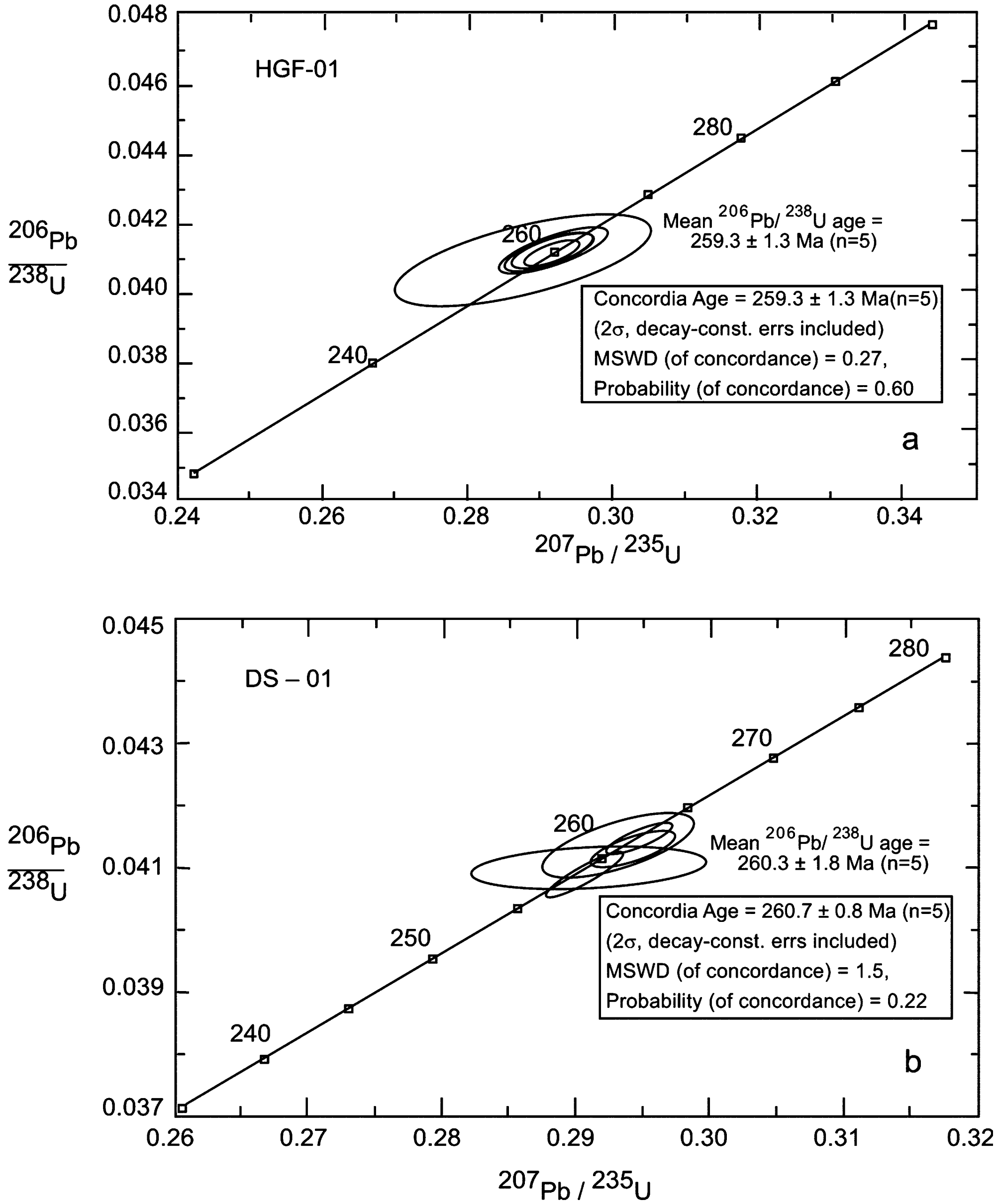

Fig. 3 Concordia diagrams showing data for **a** zircons from gabbro sample HGF-01 from the Hongge intrusion and **b** zircons from hornblende gabbro sample DS-01 from the Binggu intrusion

and unmineralized mafic/ultramafic layered intrusions in the Pan-Xi area were emplaced at ca. 260 Ma.

Our recent study indicates that the distribution of the Hongge intrusion is linked to the location of the maximum thickness of comagmatic lava, and associated with the N–S trending Xigeda fault. The fault is considered to have acted as an open-system conduit for the magmas and as a locus for the intrusion (Zhong et al. 2005). Furthermore, because of their similarities in major element, trace element, and Sr–Nd isotopic characteristics, the Hongge and Xinjie intrusions can be also correlated with units in the associated high Ti Emeishan basalts sequence (Zhong et al. 2004; Zhong et al. 2005). As described above, the Hongge and Binggu intrusions intruded the volcanic cycle II of the Emeishan basalts but did not cut through the upper cycles, which is supported by the observation that the two intrusions merely contain fragments from the lower cycle of the Emeishan basalts (Fig. 2b; SBGMR 1991; BGMRSP 1995). It is therefore suggested that the Hongge and Binggu intrusions postdate the lower flood basalt sequence but are slightly older than the upper volcanic sequence in the Pan-Xi area.

The ELIP is considered to originate from a mantle plume, which resulted in a volcanic episode producing enormous volumes of lava within a relatively short time span (Chung and Jahn 1995; Chung et al. 1998). Several magnetostratigraphic studies suggest that the Emeishan basalts were mainly erupted in one normal-polarity episode, thereby implying rapid emplacement (<2 Ma; Huang and Opdyke 1998; Ali et al. 2002). Biostratigraphic and sedimentologic investigations also reveal that there might be a time interval of <3 Ma between the regional doming-uplift related to the ELIP and rapid eruption of vast volumes of flood basalt (He et al. 2003). A very wide range of $^{40}Ar/^{39}Ar$ ages (42–256 Ma) and complicated age spectra have been reported for the Emeishan basalts and intrusive rocks. Unfortunately, the western and southwestern margins of the Yangtze block have been highly tectonized and metamorphosed during the Mesozoic and Cenozoic, which may cause varying degrees of thermal resetting (Boven et al. 2002; Lo et al. 2002; Ali et al. 2004). These ages are also in conflict with a number of stratigraphic constraints, particularly the observation that the Emeishan basalts are unequivocally older than the end of the Wuchiapingian or Dzhulfian stage (Courtillot et al. 1999; Ali et al. 2002). In addition, the bias of ca. 1% between K(Ar)/Ar and U/Pb isotopic ages (Min et al. 2000; Mundil et al. 2001) has been addressed with U/Pb ages being systematically older (most likely because of a miscalibration of the ^{40}K decay constant). Furthermore, a U/Pb zircon age of ca. 260 Ma was recently given for the base of the Wuchiapingian (Mundil et al. 2004), implying that the main eruptive age of the Emeishan basalts is older than 260 Ma. Our new age also establishes the onset of the Emeishan flood-basalt volcanism as slightly before 260 Ma, which coincide with the previous regional biostratigraphic (Sheng and Jin 1994), stratigraphic (Courtillot et al. 1999), and magneto-biostratigraphic (Ali et al. 2002) documentation, suggesting that the Emeishan basalt emission occurred at the end of the Middle Permian (end-Guadalupian).

In summary, the mineralized and unmineralized mafic/ultramafic intrusions in the Pan-Xi area are almost coeval with the Emeishan flood basalts due to the short duration of Emeishan flood volcanism, which were both produced by the same mafic–igneous event associated with the upwelling of the Emeishan mantle plume at ca. 260 Ma.

Acknowledgements We thank Prof. Hui-Min Li for his help with analytical work and the Geological Team 106 for their assistance with the fieldwork. Thorough and constructive reviews by Dr. M. Chiaradia and an anonymous reviewer are greatly appreciated. This study was financially supported by the "CAS Hundred Talents" Foundation of the Chinese Academy of Sciences to HZ, the National Natural Science Foundation of China (40473025), and by a grant from the Knowledge-innovation Program of the Chinese Academy of Sciences (KZCX3-SW-125).

References

Ali JR, Thompson GM, Song XY, Wang Y (2002) Emeishan basalts (SW China) and the 'end-Guadalupian' crisis: magnetobiostratigraphic constraints. J Geol Soc (Lond) 159:21–29

Ali JR, Lo CH, Thompson GM, Song XY (2004) Emeishan basalt Ar–Ar overprint ages define several tectonic events that affected the western Yangtze platform in the Mesozoic and Cenozoic. J Asian Earth Sci 23:163–178

BGMRSP (Bureau of Geology and Mineral Resources of Sichuan Province) (1995) Report of Regional Geology Survey (in Chinese), p 286

Boven A, Pasteels P, Punzalan LE, Liu J, Luo X, Zhang W, Guo Z, Hertogen J (2002) ^{40}Ar/^{39}Ar geochronological constraints on the age and evolution of Permo–Triassic Emeishan Volcanic Province, southwestern China. J Asian Earth Sci 20:157–175

Chung SL, Jahn BM (1995) Plume–lithosphere interaction in generation of the Emeishan flood basalts at the Permian–Triassic boundary. Geology 23:889–892

Chung SL, Jahn BM, Wu GY, Lo C H, Cong B L (1998) The Emeishan flood basalt in SW China: a mantle plume initiation model and its connection with continental break-up and mass extinction at the Permian–Triassic boundary. In: Flower MFJ, Chung SL, Lo CH, Lee TY (eds) Mantle dynamics and plate interaction in East Asia, vol. 27. American Geophysical Union, Geodynamic Series, pp 47–58

Cong BL (1988) Formation and evolution of the Pan-Xi paleorift (in Chinese). Science, Beijing, p 424

Courtillot V, Jaupart C, Manighetti I, Tapponnier P, Besse J (1999) On causal links between flood basalts and continental breakup. Earth Planet Sci Lett 166:177–195

Fan WM, Wang YJ, Peng TP, Miao LC, Guo F (2004) Ar–Ar and U–Pb geochronology of the basalts in the western Guangxi province and constraints on the eruption ages of the Emeishan basalts. Chin Sci Bull 49:1892–1900

Guo F, Fan WM, Wang YJ, Li CW (2004) When did the Emeishan mantle plume activity start? Geochronological and geochemical evidence from ultrmafic–mafic dikes in southwestern China. Int Geol Rev 46:226–234

He B, Xu YG, Chung SL, Xiao L, Wang Y (2003) Sedimentary evidence for a rapid crustal doming prior to the eruption of the Emeishan flood basalts. Earth Planet Sci Lett 213:389–405

Huang KN, Opdyke ND (1998) Magnetostratigraphic investigations on an Emeishan basalt section in western Guizhou province, China. Earth Planet Sci Lett 163:1–14

Krogh TE (1973) A low-contamination method for hydrothermal decomposition of zircon and extraction of U and Pb for isotopic age determinations. Geochim Cosmochim Acta 37:485–494

Krogh TE (1982) Improved accuracy of U–Pb zircon ages by the creation of more concordant systems using an air abrasion technique. Geochim Cosmochim Acta 46:637–649

Liang YB, Liu TY, Song GR, Jin ZM (1998) Platinum group element deposits in China (in Chinese). Metallurgical Industry, Beijing, p 185

Liu D, Shen FK, Zhang GZ (1985) Layered intrusions of the Panxi area, Sichuan province. In: Zhang YX (ed) Corpus of the Panxi paleorift studies in China (in Chinese). Geological Publishing House, Beijing, pp 85–118

Lo CH, Chung SL, Lee TY, Wu GY (2002) Age of the Emeishan flood magmatism and relations to Permian–Triassic boundary events. Earth Planet Sci Lett 198:449–458

Luo ZL, Jin YZ, Zhao XK (1990) The Emei taphrogenesis of the upper Yangtze Platform in south China. Geol Mag 127:393–405

Ma YX, Liu JD, Wang HF, Mao YS, Ji XT, Wang DK, Kan ZZ (2001) Geology of the Panzhihua region (in Chinese). Sichuan Science and Technology Press, Chengdu, p 367

Min K, Mundil R, Renne PR, Ludwig, KR (2000) A test for systematic errors in ^{40}Ar/^{39}Ar geochronology through comparison with U/Pb analysis of a 1.1 Ga rhyolite. Geochim Cosmochim Acta 64:73–98

Mundil R, Metcalfe I, Ludwig KR, Renne PR, Oberli F, Nicoll RS (2001) Timing of the Permian–Triassic biotic crisis: implications from new zircon U/Pb age data (and their limitations). Earth Planet Sci Lett 187:131–145

Mundil R, Ludwig KR, Metcalfe I, Renne PR (2004) Age and timing of the Permian mass extinctions: U/Pb dating of closed-system zircons. Science 305:1760–1763

Pirajno F (2004) Hotspots and mantle plumes: global intraplate tectonics, magmatism and ore deposits. Mineral Petrol 82:183–216

SBGMR (Sichuan Bureau of Geology and Mineral Resources) (1991) Regional geology of Sichuan province (in Chinese). Geological Publishing House, Beijing, p 680

Sheng J, Jin Y (1994) Correlation of Permian deposits in China. Palaeoworld 4:14–113

Song XY, Zhou MF, Hou ZQ, Cao ZM, Wang YL, Li YG (2001) Geochemical constraints on the mantle source of the upper Permian Emeishan continental flood basalts, southwestern China. Int Geol Rev 43:213–225

Song XY, Zhou MF, Cao ZM, Sun M, Wang YL (2003) Ni–Cu–(PGE) magmatic sulfide deposits in the Yangliuping area, Permian Emeishan igneous province, SW China. Miner Depos 38:831–843

Stanley SM, Yang X (1994) A double mass extinction at the end of the Paleozoic era. Science 266:1340–1344

Xu YG, Chung SL, Jahn BM, Wu GY (2001) Petrologic and geochemical constraints on the petrogenesis of Permian–Triassic Emeishan flood basalts in southwestern China. Lithos 58:145–168

Xu YG, He B, Chung SL, Menzies MA, Frey FA (2004) Geologic, geochemical, and geophysical consequences of plume involvement in the Emeishan flood-basalt province. Geology 32:917–920

Yao PH, Wang KN, Du CL, Lin ZT, Song X (1993) Records of China's iron ore deposits (in Chinese). Metallurgic Industry Press, Beijing, pp 633–649

Yuan HH, Zhang SF, Zhang P, Liu D, Shi ZM, Shen FK, Zhou BF, Wang MK (1985) Isotopic geochronology of the magmatic rocks in the Panxi paleorift. In: Zhang YX (ed) Corpus of the Panxi paleorift studies in China (in Chinese). Geological Publishing House, Beijing, pp 241–257

Zhang ZQ, Lu JR, Tang SH (1999) Sm-Nd ages of the Panxi layered basic-ultrabasic intrusions in Sichuan (in Chinese). Acta Geol Sin 73:263–271

Zhong H, Zhou XH, Zhou MF, Sun M, Liu BG (2002) Platinum-group element geochemistry of the Hongge Fe–V–Ti deposit in the Pan-Xi area, southwestern China. Miner Depos 37:226–239

Zhong H, Yao Y, Prevec SA, Wilson AH, Viljoen MJ, Viljoen RP, Liu BG, Luo YN (2004) Trace-element and Sr–Nd isotopic geochemistry of the PGE-bearing Xinjie layered intrusion in SW China. Chem Geol 203:237–252

Zhong H, Hu RZ, Wilson AH, Zhu WG. (2005) Review of the link between the Hongge layered intrusion and Emeishan flood basalts, southwest China. Int Geol Rev 47:971–985

Zhou MF, Malpas J, Song XY, Robinson PT, Sun M, Kennedy AK, Lesher CM, Keays RR (2002) A temporal link between the Emeishan large igneous province (SW China) and the end-Guadalupian mass extinction. Earth Planet Sci Lett 196: 113–122

Zhou MF, Robinson PT, Lesher CM, Keays RR, Zhang CJ, Malpas J (2005) Geochemistry, petrogenesis and metallogenesis of the Panzhihua gabbroic layered intrusion and associated Fe–Ti–V oxide deposits, Sichuan province, SW China. J Petrol 46: 2253–2280